Proc. 4th Int. Symp. Turbulence and Shear Flow Phenomena
Williamsburg, Virginia, June 27-29, 2005, pp. 307-312.

NOVEL TURBULENCE CONTROL STRATEGY FOR SIMULTANEOUSLY ACHIEVING FRICTION DRAG REDUCTION AND HEAT TRANSFER AUGMENTATION

Koji Fukagata, Kaoru Iwamoto[*], and Nobuhide Kasagi
Department of Mechanical Engineering,
The University of Tokyo
Hongo 7-3-1, Bunkyo-ku, Tokyo 113-8656, Japan
fukagata@thtlab.t.u-tokyo.ac.jp

ABSTRACT

An attempt is made for simultaneous, but independent control of skin friction reduction and heat transfer enhancement in a turbulent channel flow. First, a mathematical relation is derived of the contribution of turbulent heat flux to the Nusselt number. Two different thermal boundary conditions are considered: (1) isothermal condition, where two walls are kept at constant, but different temperatures; (2) isoflux condition, where both walls are heated at a given wall heat flux. By utilizing the difference between the derived relation and the similar relation for the skin friction (Fukagata et al., 2002), a strategy for the simultaneous control is proposed. The effects of the control strategy are examined by means of direct numerical simulation.

INTRODUCTION

Active feedback control is expected to play a significant role in reducing the skin friction drag in wall-bounded turbulent flows and has been widely studied both theoretically (see, e.g., Kasagi (1998) and Kim (2003), for review) and experimentally (Rathnasingham and Breuer (2003); Suzuki et al. (2005)). With this control technique, heat transfer characteristics of turbulent flows can also be drastically modified. In many industrial applications, such as heat exchangers and piping systems, it is desirable to keep the skin friction drag reasonably small. As for the heat transfer, either enhancement or suppression is preferred depending on the function of equipment.

One of the important focal points in the previous DNS studies on the turbulent heat transfer was the similarity between momentum and heat transport. According to these studies, the degree of similarity when the Prandtl number is around unity ($Pr \sim 1$) seems to strongly depend on the wall boundary condition for the thermal field. A strong similarity exists when the heat is uniformly generated in the channel (Kim and Moin, 1989) and when the isoflux condition is applied on the walls (Kasagi et al., 1992; Tiselj et al., 2001). When two walls are kept at constant, but different temperatures, the similarity is strong in the regions near the wall, but weaker in the core region of channel (Lyons et al., 1991; Seki et al., 2003).

Due to the above-mentioned similarity between momentum and heat transport, simultaneous reduction of skin friction and heat transfer is straightforward. For simultaneous achievement of skin friction reduction and heat transfer enhancement, however, no control strategy has been established. An attempt of such a dissimilar control was once made by Yokoo et al., (2000) for a turbulent channel flow with isothermal walls kept at different temperatures. They set a cost function including both the skin friction and wall heat flux and used the optimal control procedure to determine the control input, i.e., blowing/suction from the wall, so that the cost function is minimized. Despite the huge computational cost required for the optimization, the effect of control was very small. In the best case, they attained 0.006% heat transfer augmentation with 0.002% drag reduction.

In the present study, a similar attempt is made from a different point of view. First, a mathematical relationship is derived of the contribution of turbulent heat flux to the Nusselt number. By utilizing the difference between the derived relation and the corresponding relationship for the skin friction (Fukagata et al., 2002), a strategy for the simultaneous control is proposed. A control scheme is then developed based on the proposed strategy and its effects if examined by DNS.

CONTRIBUTION OF TURBULENT HEAT FLUX TO NUSSELT NUMBER

First, an explicit mathematical relation is derived of laminar and turbulent contributions to the Nusselt number in a fully developed turbulent channel flow.

The transport equation of the temperature, T^*, can be written as

$$\frac{\partial T^*}{\partial t} = -\frac{\partial (u_j T^*)}{\partial x_j} + \frac{1}{Re_b Pr}\frac{\partial^2 T^*}{\partial x_j^2} \ . \tag{1}$$

Throughout the paper, the subscript of $*$ denotes dimensional variables. The length, velocity, and time in Eq. (1) are nondimensionalized by the channel half-width, δ^* and twice the bulk mean velocity, $2U_b^*$.

The bulk Reynolds number and the Prandtl number are defined, respectively, by

$$Re_b = \frac{2U_b^*\delta^*}{\nu^*} \tag{2}$$

and

$$Pr = \frac{\nu^*}{\alpha^*} \ , \tag{3}$$

where α^* is the thermal diffusivity, which is assumed to be constant.

[*]Present address: Department of Mechanical Engineering, Faculty of Science and Technology, Tokyo University of Science, Yamazaki 2641, Noda, Chiba 278-8510, Japan.

Two different thermal boundary conditions are considered:

1. constant, but different temperatures on two walls (isothermal wall condition);

2. constant heat flux on two walls (isoflux wall condition).

In both cases, temperature fluctuation is assumed to be zero on the walls. In the first case, one wall is heated and the other is cooled, so that they are kept at given (different) temperatures. The problem is to obtain the wall heat flux under the given temperature difference. In the second case, both walls are heated by a given wall heat flux. The temperature difference is determined as a result of turbulent heat transport. Due to this difference in the problem setting, the quantity used for the nondimensionalization should also be different in each case. Therefore, the derivation process for each case is separately presented below.

Isothermal condition

We consider a fully developed channel flow, as shown in Fig. 1(a). The two channel walls are kept at constant temperatures, $T^*|_{y=0}$ and $T^*|_{y=2}$. The temperature difference, ΔT^*, is defined as

$$\Delta T^* = T^*|_{y=1} - T^*|_{y=0} = T^*|_{y=2} - T^*|_{y=1} \ . \qquad (4)$$

By using this given temperature difference, a dimensionless temperature, ϑ, is defined as

$$\vartheta = \frac{T^* - T^*|_{y=1}}{\Delta T^*} \ . \qquad (5)$$

The transport equation for the dimensionless mean temperature reads

$$0 = -\frac{d\overline{v'\vartheta'}}{dy} + \frac{1}{Re_b Pr}\frac{d^2\overline{\vartheta}}{dy^2} \ . \qquad (6)$$

Here, the overbar denotes the average in homogeneous (i.e., the streamwise and spanwise) directions and in time. The prime denotes the fluctuation components. The boundary conditions are

$$\vartheta|_{y=0} = -1 \ , \quad \vartheta|_{y=2} = 1 \ . \qquad (7)$$

Note that the dimensionless bulk-mean temperature is zero, because the mean velocity profile is symmetric and the mean temperature profile is anti-symmetric around the center plane.

The Nusselt number is defined as

$$Nu = \frac{D_h^*}{\Delta T^*}\frac{q_w^*}{\lambda^*} = \frac{4\delta^*}{\Delta T^*}\left.\frac{d\overline{T}^*}{dy^*}\right|_w = 4\left.\frac{d\overline{\vartheta}}{dy}\right|_w \ , \qquad (8)$$

where λ^* is the heat conduction coefficient, D_h^* is the hydraulic diameter, and the subscript of w denotes the quantity on the wall. It should be stressed that the amount of wall heat flux, q_w^*, is determined as a result of turbulent heat transport. Due to the anti-symmetry of the mean temperature profile, the mean heat flux is the same on the both walls, i.e.,

$$Nu = 4\left.\frac{d\overline{\vartheta}}{dy}\right|_{y=0} = 4\left.\frac{d\overline{\vartheta}}{dy}\right|_{y=2} \ . \qquad (9)$$

By integrating Eq. (6) once from 0 to y, we obtain

$$\frac{Nu}{4Re_b Pr} = -\overline{v'\vartheta'} + \frac{1}{Re_b Pr}\frac{d\overline{\vartheta}}{dy} \ , \qquad (10)$$

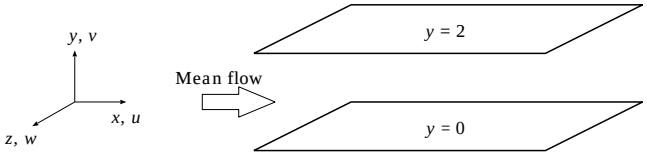

Figure 1: Flow geometry.

where $\overline{v'\vartheta'}|_{y=0} = 0$ and Eq. (9) were used. This integration is equivalent to obtain the flux balance. Equation (10) is integrated again from 0 to 1 to read

$$\frac{Nu}{4Re_b Pr} = \int_0^1 (-\overline{v'\vartheta'})dy + \frac{1}{Re_b Pr} \ . \qquad (11)$$

Here, the boundary condition, i.e., $\overline{\vartheta}|_{y=0} = -1$ and the anti-symmetry condition, i.e., $\overline{\vartheta}|_{y=1} = 0$, were used. Hence,

$$Nu = 4 + 4Re_b Pr \int_0^1 (-\overline{v'\vartheta'})dy \ . \qquad (12)$$

Note that, due to anti-symmetry of the mean temperature, the same relation can be obtained when the integration is started from y to 2.

The derived relation, Eq. (12), suggests that the Nusselt number can be decomposed into two parts. The first term in the right hand side is the laminar contribution, which is identical to heat conduction, and the second term is the turbulent contribution. The turbulent contribution is a simple integration of turbulent heat flux, $(-\overline{v'\vartheta'})$, This is clearly different from the turbulent contribution to the skin friction coefficient, which is given by a weighted integration of the Reynolds shear stress (Fukagata et al., 2002), i.e.,

$$C_f = \frac{12}{Re_b} + 12\int_0^2 (1-y)(-\overline{u'v'})\,dy \ . \qquad (13)$$

Isoflux condition

In this case, the constant wall heat flux, q_w^*, is the given condition. Therefore, we introduce another dimensionless temperature, θ (which is different from ϑ above), i.e.,

$$\theta = \frac{T_w^* - T^*}{\Delta T_x^*} \ , \qquad (14)$$

where $T_w^*(x)$ is the wall temperature, which linearly varies along the streamwise direction. From the global heat balance, the reference temperature of ΔT_x^* is found to be the change of T_w^* (and also the bulk mean temperatures, T_b^*) over the streamwise distance of $\delta^*/2$, i.e.,

$$\Delta T_x^* = \frac{\delta^*}{2}\frac{dT_w^*}{dx^*} = \frac{\delta^*}{2}\frac{dT_b^*}{dx^*} = \frac{q_w^*}{\rho^* c_p^*(2U_b^*)} \ . \qquad (15)$$

By using this nondimensionalization, the transport equation for the dimensionless mean temperature reads

$$0 = -\frac{d\overline{v'\theta'}}{dy} + \frac{1}{Re_b Pr}\frac{d^2\overline{\theta}}{dy^2} + 2\overline{u} \ . \qquad (16)$$

The last term in Eq. (16) corresponds to the source term, $\overline{u}(dT_w^*/dx)$ (Kasagi et al., 1992). The boundary conditions are

$$\theta|_{y=0} = 0 \ , \qquad \theta|_{y=2} = 0 \ . \tag{17}$$

Integration of Eq. (16) from $y = 0$ to $y = 1$ gives the global heat balance, i.e.,

$$0 = -\frac{1}{Re_b Pr} \left. \frac{d\overline{\theta}}{dy} \right|_w + 1 \ . \tag{18}$$

Note that the mean temperature is symmetric with respect to the center plane. Therefore, the Nusselt number is expressed as

$$Nu = \frac{D_h^*}{\Delta T^*} \frac{q_w^*}{\lambda^*} = \frac{-4 \left. \frac{dT^*}{dy} \right|_w}{T_w^* - T_b^*} = \frac{4}{\Theta_b} \left. \frac{d\overline{\theta}}{dy} \right|_w = \frac{4 Re_b Pr}{\Theta_b} \ , \tag{19}$$

where $\Theta_b = (T_w^* - T_b^*)/\Delta T_x^*$ is the dimensionless bulk mean temperature.

Under the present thermal boundary conditions, the derivation of the relationship between Nu and $-\overline{v'\theta'}$ is exactly the same as that for the skin friction (Fukagata et al., 2002). Namely, we apply triple integration, i.e., $\int_0^1 \overline{u} dy \int_0^y dy \int_0^y dy$, to Eq. (16). The first integration essentially gives the flux balance. The second leads to the mean temperature profile. The third is akin to obtaining the bulk mean temperature from the temperature profile. By transforming multiple integrations to single integrations by applying the integration by parts, it results in

$$\frac{1}{Nu} = \frac{1}{4} - \frac{1}{4} \int_0^1 (1-\phi)(-\overline{v'\theta'}) dy - \frac{1}{4} \int_0^1 \phi(2-\phi) dy \ , \tag{20}$$

where $\phi(y)$ is defined as

$$\phi(y) = 2 \int_0^y \overline{u}(\eta) d\eta \ , \tag{21}$$

and referred to here as the fractional flow rate. Unlike that for the skin friction, i.e., Eq. (13), or that in the isothermal case, i.e., Eq. (12), the relationship appears as the inverse of Nusselt number. This is due to the fact that the quantity that determines the Nusselt number, i.e., the dimensionless bulk mean velocity (Θ_b), has an inverse relation to Nu, as can be noticed in Eq. (19). Moreover, this inverse relation originates from the problem setting to obtain $\Delta T^* \propto Nu^{-1}$ for a given $q_w^* \propto Nu$, which is on the contrary to the case of Eq. (13), where the problem is to obtain $\tau_w^* \propto C_f$ for a given $U_b^* \propto C_f^{-1/2}$.

The derivation is not complete in the sense to decompose into laminar and turbulent contributions, because the third term (which originates from the source term in Eq. (16)) also includes the contribution from the laminar flow. Therefore, we decompose the mean temperature, $\overline{\theta}$, into the laminar profile, $\overline{\theta}_L$ and the deviation from that, $\overline{\theta}_T$, i.e.,

$$\overline{u} = \overline{u}_L + \overline{u}_T \ , \tag{22}$$

where

$$\overline{u}_L(y) = \frac{3y}{4}(2-y) \ . \tag{23}$$

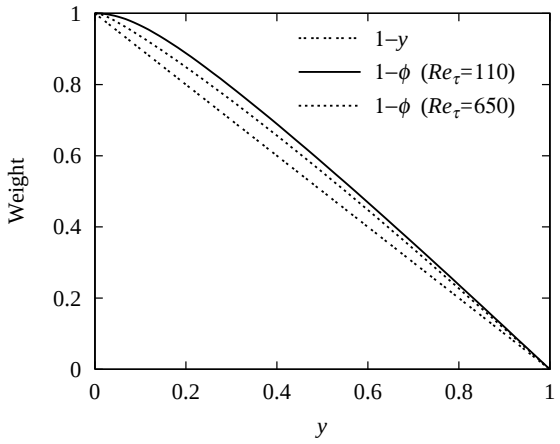

Figure 2: Weighting functions in the turbulent contribution term, $(1-y)$ for the skin friction and $(1-\phi)$ for the heat transfer in the isoflux case. The values of ϕ at different Reynolds numbers are computed using the DNS data by Iwamoto et al. (2002).

The deviation part, $\overline{u}_T$, can be calculated by using Eq. (13) as

$$\begin{aligned} \overline{u}_T(y) \quad = \quad & Re_b \left[\frac{3y}{4}(2-y) \int_0^1 2(1-\eta)(-\overline{u'v'}) d\eta \right. \\ & \left. - \int_0^y (-\overline{u'v'}) d\eta \right] \ . \end{aligned} \tag{24}$$

Similarly, the fractional flow rate, ϕ, is decomposed into

$$\phi = \phi_L + \phi_T \ , \tag{25}$$

where

$$\phi_L(y) = 2 \int_0^y \overline{u}_L(\eta) d\eta = \frac{y^2}{2}(3-y) \ , \tag{26}$$

and

$$\phi_T(y) = 2 \int_0^y \overline{u}_T(\eta) d\eta \ . \tag{27}$$

By using this decomposition, the rest of the laminar contribution can be extracted from the last term in Eq. (20), i.e.,

$$\begin{aligned} -\frac{1}{4} \int_0^1 \phi(2-\phi) dy \quad = \quad & -\frac{9}{70} - \frac{1}{4} \int_0^1 [(y^3 - 3y^2 + 2)\phi_T \\ & - \phi_T^2] dy \ . \end{aligned} \tag{28}$$

Thus, the relationship for the Nusselt number can finally be expressed as

$$\begin{aligned} \frac{1}{Nu} \quad = \quad & \frac{17}{140} - \frac{1}{4} \int_0^1 (1-\phi)(-\overline{v'\theta'}) dy \\ & - \frac{1}{4} \int_0^1 [(y^3 - 3y^2 + 2)\phi_T - \phi_T^2] dy \ . \end{aligned} \tag{29}$$

The first term in Eq. (29) corresponds to the heat transfer in a laminar channel flow with isoflux walls, i.e., $Nu =$

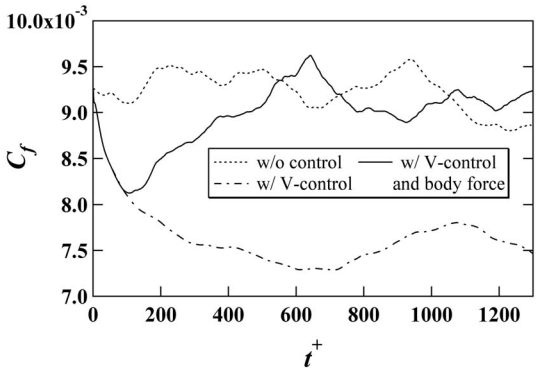

Figure 3: Time trace of C_f in the isothermal case.

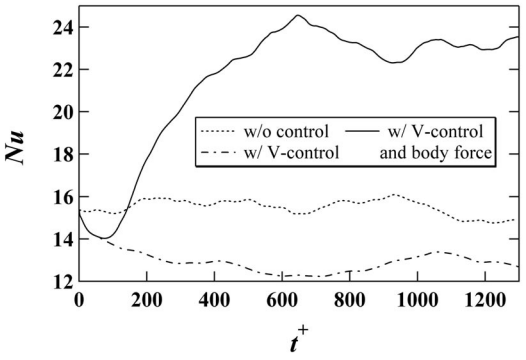

Figure 4: Time trace of Nu in the isothermal case.

$140/17 \simeq 8.235$, which is a well-known value (see, e.g., Kays and Crawford, 1993). The second term represents the contribution from the turbulent heat flux. This term is usually positive in a turbulent channel flow, which results in reduction of $1/Nu$ (i.e., increase of Nu) as compared to that of laminar flow. The last contribution is determined solely by the velocity profile due to the presence of the Reynolds shear stress, as can be noticed from Eq. (24).

CONTROL STRATEGY

Based on the derived relations, control strategies are proposed for two different boundary conditions considered here.

In the case of isothermal walls with different temperature, the difference in the weighting functions for the skin friction, Eq. (13), and heat transfer, Eq. (12), i.e., $(1-y)$ and 1, in the turbulent contribution term suggests that simultaneous control of drag reduction and heat transfer augmentation may be possible, if the turbulence is suppressed near the wall and enhanced in the central region of the channel.

In the case of constant heat flux from both walls, the derived relationship indicates the difficulty of simultaneous achievement of friction drag reduction and heat transfer augmentation. As shown in Fig. 2, the weighting function in the turbulent contribution term for the heat transfer, i.e., $1-\phi$, has a distribution quite close to that of the turbulent contribution term for the skin friction, i.e., $1-y$. The difference in the weighting functions becomes smaller as the Reynolds number increases, as is also shown in the figure. Despite this implication, a possible control strategy may be to enhance the turbulence a bit far from the wall, say from $y = 0.3$ to 0.6. The effect of control, however, may be much weaker than that expected in the above-mentioned isothermal case.

Note that the third term in Eq. (29) has also non-negligible contribution to the Nusselt number. Evaluation using the available DNS database (http://www.thtlab.t.u-tokyo.ac.jp/), however, suggests that it is considerably smaller than the turbulent contribution term.

VERIFICATION OF THE PROPOSED STRATEGY

The proposed strategy is examined by means of DNS of channel flow at $Re_b = 3220$ (i.e., $Re_\tau = 110$ in uncontrolled flow) and $Pr = 0.71$. The DNS code is based on the pseudo-spectral method (Iwamoto et al, 2002) .

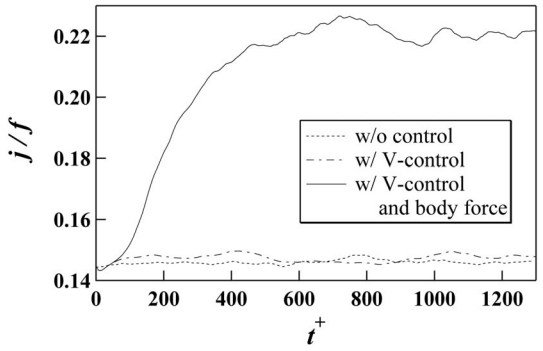

Figure 5: Time trace of j/f factor in the isothermal case.

The opposition control scheme (Choi et al., 1994) is adopted for the suppression of near-wall Reynolds stress. The virtual detection plane is set at $y_d^+ = 10$. In addition, a virtual body force, i.e., $-\beta f(y)\theta'$, is added to the wall-normal momentum equation for the enhancement of turbulent heat-flux in the central region of the channel. Here, β is an amplitude coefficient and $f(y)$ is an envelope function.

First, the case of isothermal walls with different temperature is examined. According to the strategy above, the envelope function is set to have a value of unity in the central region away from the wall and zero near the wall: $f(y) = 1$ for $0.5 < y < 1.5$; $f(y) = 0$ for $0 < y < 0.5$ and $1.5 < y < 2$. The amplitude coefficient is set at $\beta = 7.4$ (nondimensionalized by using $2U_b^*$, δ^* and ΔT^*).

Figures 3 and 4 show the time traces of the skin friction coefficient (C_f) and the Nusselt number (Nu) in three cases: 1) without control, 2) with opposition control, 3) with opposition control and body force (referred to as present control). Both C_f and Nu decrease just after the onset of present control. The time traces of these closely follow those with opposition control only (denoted as w/V-control). In the later time, both C_f and Nu increase. This complicated behavior is attributed to two different time scales in different regions: the short time scale in the region near the wall, which corresponds to the direct effect of opposition control (Fukagata and Kasagi, 2003); and the long time scale in the region near the wall, which reflects the effect of forcing in the central region of the channel. After the initial transience, C_f returns to the level of uncon-

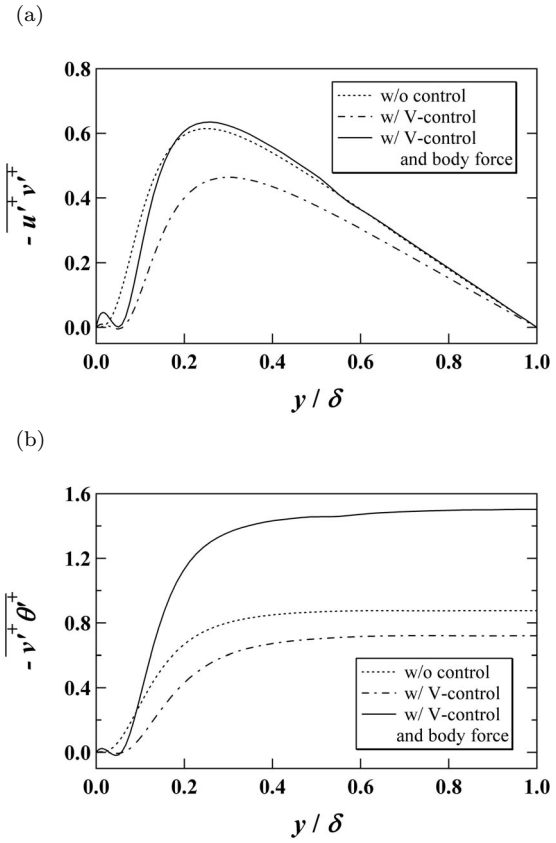

Figure 6: Turbulence statistics in the isothermal case. (a) Reynolds shear stress; (b) turbulent heat flux.

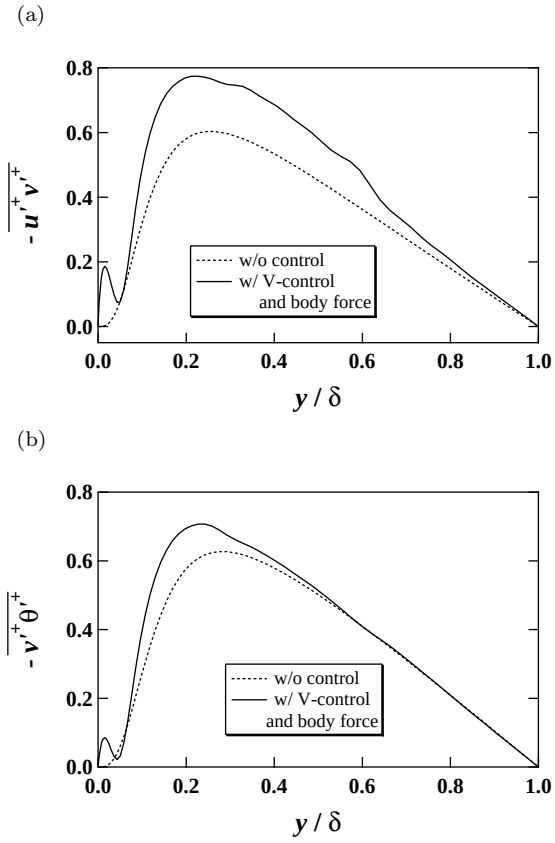

Figure 8: Turbulence statistics in the isoflux case. (a) Reynolds shear stress; (b) turbulent heat flux.

trolled flow, and Nu further increase to about 1.5 times of that of the uncontrolled flow. As the measure of heat transfer performance, j/f factor (where $j = Nu/(Re_b\ Pr^{1/3})$ and $f = 4C_f$) is shown in Fig. 5. The heat transfer performance is improved by 50 % with the present control.

The profiles of Reynolds shear stress and turbulent heat flux exhibit the changes that we expected, as shown in Fig. 6. The Reynolds shear stress profile with the present control is roughly similar to that in the uncontrolled case. This is consistent with the observation that C_f takes approximately the same value as the that in the uncontrolled case. The turbulent heat flux is suppressed near the wall ($y/\delta < 0.1$), whereas largely enhanced in the central region of the channel. This change leads to significant increase in the Nusselt number, as implied by Eq. (12).

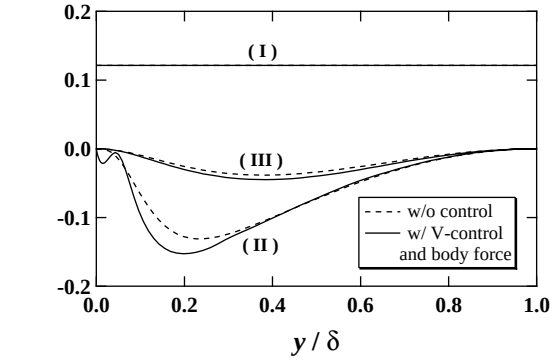

Figure 7: Fractional contribution to $(1/Nu)$ in the isoflux case. (I), laminar contribution, i.e., 17/140; (II), turbulent contribution; (III), the third term in Eq. (29).

Subsequently, the case of isoflux walls is examined. In this case, the envelope function is set to have the value of $f(y) = 1$ for $0.3 < y < 0.6$ and $1.4 < y < 1.7$, where the weighting functions for the Reynolds shear stress and turbulent heat flux have relatively large differences ($f(y) = 0$ in the other region). The amplitude coefficient is set at $\beta = 0.0013$ (nondimensionalized by using $2U_b^*$, δ^* and ΔT_x^*). Note that we examined several values of β larger than 0.0013. In those cases, however, the computations became unstable due to the rapid increase of skin friction, i.e., increase of turbulence level beyond the grid resolution, and the flow fields did not reach quasi-steady states.

The resultant skin friction coefficient and the Nusselt number are, respectively, 1.22 and 1.25 times larger than those of the uncontrolled flow. The increase of corresponding j/f factor is about 2%. As was expected from Eq. (29) and Fig. 2, the effect of control is very small.

Figure 7 shows the fractional contributions to the inverse of Nusselt number (i.e., the integrand of each term in Eq. (29)) as functions of y. It is clearly illustrated that the modification of turbulent heat flux around $y/\delta = 0.2$ contributes to the increase of Nusselt number. It is also confirmed that the third

term in Eq. (29) less contributes to the Nusselt number.

The profiles of Reynolds shear stress and the turbulent heat flux are shown in Fig. 8. Both of these quantities are largely suppressed around $y^+ \simeq 5$, which corresponds to the location of virtual wall (Hammond et al., 1998), due to the opposition control. The turbulence is enhanced by the body force in the region of $0.3 < y < 0.6$. The amounts of increase in this region, however, are not equal for the Reynolds shear stress and the turbulent heat flux: the increase of the Reynolds shear stress is much larger than that of the turbulent heat flux. These dissimilar modifications make the control effect even smaller.

Another reason for the small control effect might be the very low Reynolds number used in the simulation ($Re_\tau = 110$). In the present case, the regions where the turbulence is suppressed ($0 < y^+ < 10$) and where it is enhanced ($0.3 < y < 0.6$, i.e., $33 < y^+ < 66$) are too close to each other. The weighting functions in turbulent contribution terms are scaled by δ (strictly speaking, the weighting function for the heat flux has a weak dependence on the Reynolds number, too). Therefore, there is a possibility for the present control to be more effective at a higher Reynolds number, where the suppression and enhancement regions become far apart. Verification of the present control strategy at a higher Reynolds number, however, remains for a future study.

CONCLUSIONS

We derived analytical relationships between the Nusselt number and the turbulent heat flux distribution for two different thermal boundary conditions.

In the case with isothermal walls kept at different temperatures, the Nusselt number can be clearly decomposed into the laminar and turbulent contributions. The turbulent contribution is proportional to an integration of the turbulent heat flux. This relationship, together with the corresponding relationship for the skin friction (Fukagata et al., 2002), suggests that the near-wall turbulence should be suppressed and far-wall turbulence should be enhanced in order to achieve simultaneous achievement of skin friction reduction and heat transfer enhancement. Direct numerical simulation with the opposition control and virtual forcing in the central region confirms the above-mentioned strategy. The heat transfer was increased about 1.5 times, while the friction was kept at the same level.

In the case of isoflux wall condition, the inverse of Nusselt number can be decomposed into three terms. The first two terms are the laminar and turbulent contributions. The third term, which originates from the source term in the dimensionless heat transport equation, is a function solely of the Reynolds shear stress. The weighting function for the turbulent heat flux in the turbulent contribution term is practically similar to that for the Reynolds shear stress in the relationship for the skin friction. Therefore, above-mentioned simultaneous control is more difficult in this case. Nevertheless, the direct numerical simulation demonstrated augmentation of heat transfer slightly larger than increase of drag, by using a control scheme similar to that used for the isothermal case.

ACKNOWLEDGMENTS

This work was supported through the Project for Organized Research Combination System by the Ministry of Education, Culture, Sports and Technology of Japan (MEXT). The first author (KF) was also, in part, supported through the 21st Century COE Program, "Mechanical Systems Innovation," by MEXT.

REFERENCES

Choi, H., Moin, P., and Kim, J., 1994, "Active Turbulence Control for Drag Reduction in Wall-Bounded Flows," *J. Fluid Mech.*, Vol. 262, pp. 75-110.

Fukagata, K., Iwamoto, K. and Kasagi, N., 2002, "Contribution of Reynolds Stress Distribution to the Skin Friction in Wall-Bounded Flows," *Phys. Fluids*, Vol. 14, pp. L73-L76.

Fukagata, K. and Kasagi, N., 2003, "Drag Reduction in Turbulent Pipe Flow with Feedback Control Applied Partially to Wall," *Int. J. Heat Fluid Flow*, Vol. 24, pp. 480-490.

Iwamoto, K., Suzuki, Y., and Kasagi, N., 2002, "Reynolds Number Effect on Wall Turbulence: Toward Effective Feedback Control," *Int. J. Heat Fluid Flow*, Vol. 23, pp. 678-689.

Hammond, E. P., Bewley, T. R., Moin, P., 1998, "Observed Mechanisms for Turbulence Attenuation and Enhancement in Opposition-Controlled Wall-Bounded Flows," *Phys. Fluids*, Vol. 10, pp. 2421-2423.

Kasagi, N., 1998, "Progress in Direct Numerical Simulation of Turbulent Transport and Its Control," *Int. J. Heat Fluid Flow*, Vol. 19, pp. 128-134.

Kasagi, N., Tomita, Y., and Kuroda, A., 1992, "Direct Numerical Simulation of Passive Scalar Field in a Two Dimensional Turbulent Channel Flow," *ASME J. Heat Transfer*, Vol. 114, pp. 598-606.

Kays, W. M., and Crawford, M. E., 1993, *Convective Heat and Mass Transfer, 3rd Edition*, McGraw-Hill Inc., New York, p. 125.

Kim, J., 2003, "Control of Turbulent Boundary Layers," *Phys. Fluids*, Vol. 15, pp. 1093-1105.

Kim, J. and Moin, P., 1989, "Transport of Passive Scalars in a Turbulent Channel Flow," *Turbulent Shear Flow 6*, Springer-Verlag, pp. 85-96.

Lyons, S. L., Hanratty, T. J., and McLaughlin, J. B., 1991, "Direct Numerical Simulation of Passive Heat Transfer in a Turbulent Channel Flow," *Int. J. Heat Mass Transfer*, Vol. 34, pp. 1149-1161.

Rathnasingham R. and Breuer K., 2003, "Active Control of Turbulent Boundary Layers," *J. Fluid Mech.*,Vol. 495, pp. 209-233.

Seki, Y., Abe, H., and Kawamura, H., 2003, "DNS of Turbulent Heat Transfer in a Channel Flow with Different Thermal Boundary Conditions," *Proc. 6th ASME-JSME Therm. Eng. Joint Conf.*, March 2003, Hawaii, TED-AJ03-226.

Suzuki, Y., Yoshino, T., Yamagami, T., and Kasagi, N., 2005, "Drag Reduction in a Turbulent Channel Flow by Using a GA-Based Feedback Control System," *Proc. 6th Symp. Smart Control of Turbulence*, March 2005, Tokyo, pp. 31-40.

Tiselj, I., Pogrebnyak, E., Li, C., Mosyak, A., and Hetsroni, G., 2001, "Effect of Wall Boundary Condition on Scalar Transfer in a Fully Developed Turbulent Flume," *Phys. Fluids*, Vol. 13, pp. 1028-1039.

Yokoo, M., Kasagi, N., and Suzuki, Y., 2000, "Optimal Control of Heat Transfer and Skin Friction in Wall Turbulence," *Proc. 3rd Int. Symp. on Turbulence, Heat and Mass Transfer*, Nagoya, 2000, pp. 949-956.